

Computed Tomography Imaging Features of Malignant “Triton” Tumor for Its Clinical Diagnosis: Report of Two Cases

Yuan Li

Chongqing Medical University

Chun Zeng

Chongqing Medical University

Ning Jiang

Chongqing Medical University

David P. Molloy

Chongqing Medical University

Qiling Peng (✉ pqlpzy@cqmu.edu.cn)

Chongqing Medical University

Cheng Zhang

Chongqing Medical University

Haoming Shi

Chongqing Medical University

Dan Chen

Chongqing Medical University

Qingchen Wu

Chongqing Medical University

Case report

Keywords: Computed tomography; Malignant triton tumors; Linear septum; Presumptive diagnosis; Neurofibromatosis type 1.

Posted Date: July 17th, 2020

DOI: <https://doi.org/10.21203/rs.3.rs-42437/v1>

License:   This work is licensed under a Creative Commons Attribution 4.0 International License.

[Read Full License](#)

Abstract

Background: malignant triton tumors (MTTs) are an extremely rare subtype of malignant periphery nerve sheave tumors (MPNSTs). Clinical diagnosis of MTTs is difficult before surgery due to its low incidence and the lack of knowledge. Therefore, to describe and summarize the computed tomography (CT) imaging characteristics of malignant triton tumors (MTTs) is of great assistance for early and preoperative diagnosis.

Case presentation: Two case reports were closely observed in our hospital, with the presumptive diagnosis of MTT by CT scan examination before surgery. The diagnosis of MTT was eventually confirmed by immunochemical (IHC) assay, which verified speculation of CT scans. Huge, irregular, well-circumscribed lobulated mass-like shadows can be observed from these patients by CT scans. Besides, heterogeneity of density within the body of tumor was well-established by CT scans, together with linear septum. Meanwhile, CT scans demonstrated that calcifications were remarkable at the margin of tumor body.

Conclusions: Some CT image features from two cases admitted to our hospital were presented as a reference for the preoperative diagnosis of MTTs: (i) enormity of mass-like shadow; (ii) presence of well-circumscribed lobulated shape; (iii) septum within the well-defined mass accompanied with hemorrhage, necrosis and cystic changes as well as calcification, especially within neurofibromatosis type 1 (NF-1) patients.

Background

Malignant schwannomas with rhabdomyosarcomatous differentiation, originally described by Masson¹ and now designated malignant "Triton" tumors (MTTs), appear as neurogenic sarcomas with skeletal muscle differentiation in squamous epithelium, bone and possibly fat tissues.² MTT is an extremely rare malignant periphery nerve sheave tumors (MPNSTs), with a worldwide incidence of fewer than 200 cases reported to date.³ Of these, 69% of MTTs have been diagnosed in young male patients with neurofibromatosis type 1 (NF-1) and 31% are sporadic cases mostly occurring in older women.⁴⁻⁵ At present, treatment scenarios for MTTs include radical surgical resection, adjuvant chemotherapy and radiation, with the latter consideration as the standard protocol for MPNST or soft tissue sarcoma.⁶⁻⁷ In respect of tumor location, MTTs primarily arise in head, neck and trunk regions, but also infrequently observed in lung, mediastinum, abdomen and prostate tissues,⁸⁻⁹ which invariably culminates with the untimely demise of the infected individual.

Recurrence of MTT after excision is common and with a 5-year survival rate of merely 12%, prognosis remains extremely unfavorable for afflicted individuals.^{4, 6, 10} Moreover, in the absence of suitable awareness and education concerning a disease of intrinsically low incidence within the general human population, pre-surgical misdiagnoses of MTT are all too frequent. Early identification and analysis of the clinic pathology of MTTs is, therefore, of critical importance. The first truly indicative criteria for a positive

diagnosis of tumorigenic MTTs were derived in 1973 and include location along a peripheral nerve ganglioneuroma, Schwann cell tumor characteristics and observation of rhabdomyoblasts within the body of tumor.¹¹ Subsequent immunohistochemical (IHC) analyses for the skeletal muscle-specific markers myogenin or Myo-D1 are then used as confirmation of malignancy.⁹ Unfortunately, assays for the presence of rhabdomyoblasts with MTTs are prone to error being reliant upon objective separation of MTTs with sample that contain significant numbers of Schwann cell that negatively stain for desmin and myogenin and/or Myo-D1.² Such investigations are further impeded as IHC assessments are performed post-surgery, although pathological evaluation still provides a reliable tool for neurogenic tumor classification.

Until recently, computed tomography scanning diagnostics for MTTs were underused. As a medical imaging procedure, multiple X-ray measurements are combined into images of specific areas within the body. This enables discernment of anatomical features to be made with high precision leading to increased accuracy of diagnosis, staging and monitoring of morphological changes in MTTs during preoperative periods. Overall, the technique is a noninvasive pre-surgical alternative for diagnosis of MTTs that ultimately allows for improvements in both palliative care and longevity of patients.

Case Presentation

The first scenario presented pertains to a 41-year-old female whom had complaints relating to progressive deterioration in thoracic distress and shortness of breath over two months prior to hospital admission. Representative hematoxylin and eosin (H&E) staining of a postoperative biopsy are presented (Fig. 1). A tumorous growth was clearly identified as a discrete mass of hyperchromatic spindle cells with indistinct cytoplasm after H&E staining. The overall architecture appeared to be either diffuse or alternate hypo-/dense-cellular regions (Fig. 1A). The tumor tissue could therefore be assigned microscopically as a malignant schwannoma of variable cellular distribution with non-homogenous rhabdomyosarcomatous features (Fig. 1B). In addition, rhabdomyoblasts with a dense eosinophilic cytoplasm and cytoplasmic cross striations were observed scattered throughout the stroma and mainly comprised of pleomorphic spindle cells (Fig. 1C). The IHC assay was positive for S-100 protein, Myo-D1 and Desmin and when combined, these findings supported a diagnosis of MTT, comparable to previous studies.³

Further confirmation for MTT was derived from preoperative CT imaging scans of the chest region which revealed the presence of a distinctive and large non-MPNSTs/soft tissue sarcoma mass of size 7.7 cm × 6.0 cm located within the medial basal segment of lower lobe of the right lung (Fig. 2A). Additional imaging analyses obtained using contrast-enhanced CT scans of the thoracic region re-affirmed the presence of an irregular hemorrhagic or necrotic, well-circumscribed lobule (Fig. 2B). A low-density cyst was also evidenced by absence of mediastinal and hilar node enlargements in the surrounding region and a distinct septate demarcation within the cellular mass at the lesion periphery (Fig. 2B). The patient was not subjected to postoperative chemo or radiotherapy and after five months appeared to have recovered sufficiently with only minor refractory movement disorders, limb numbness, backache and dysuria discomfort were noted. Initially, long-term prognosis appeared to be positive, as postoperative re-

examination of the chest area in CT scans revealed no recurrence of the mass-like shadow within the operative region. However, several well-defined and differentially sized homogeneous nodules were seen as persistent within the bilateral lungs which raised concerns of MTT metastasis and possible malignancy (Fig. 2C). Thus, further investigations of patient discomfort arising from clinical symptoms were performed through MRI upon the spinal cord. In these, a homogeneous tissue mass were observed to be expanding within the vertebral index at the 4th and 5th thoracic (T4-T5) segments causing microbleeds (Fig. 2D). Rather more radical anatomical consequences of MTT metastasis within thoracic region were also noted and included severe destruction of bone tissue on the right thoracic pedicle, plate and transverse processes of the T4 and T5 segments alongside tumor invasion of adjacent ribs, pleura and soft tissues (yellow arrow in Fig. 2D). Aside these, an outward dispersal of the lesion from the spinal dura mater and uncontrolled growth within the thoracic spinal cord were also observed (red arrow in Fig. 2D). Unfortunately, these symptoms were indicative of rapid multiple distal metastasis of MTT and the patient passed away two months later.

In a second scenario, a 37-year-old male presented with a persistent lower left quadrant dull abdominal pain over two months. There was a paternal familial predisposition of NF-1 inclusive of an uncle and grandfather. CT scanning of the abdominal region revealed the presence of a heterogeneous hemorrhagic or necrotic discoid mass 10 cm × 6.3 cm in size located within the left-side abdominal cavity (Fig. 3A). Calcifications were also evidenced in CT scans occurring at the margin of the cyst. In contrast-enhanced CT scans, the cyst margin was more prominent within the patient's chest region (Fig. 3B) and similarities to the aforementioned case with the presence of a linear septum within the cellular mass were noted (white arrow, Fig. 3B). Furthermore, an irregular hypodense nodule was observed in between the T12 and the 1st lumbar (L1) vertebral canal interspersed with the left foramen intervertebral disc of the spinal cord (Fig. 3C). The lesion also resulted in significant compression of the adjacent vertebral bodies and adnexal bones and nodule elongation. Similar nodules also appeared posterior to the pancreas body and proximal to the right iliopsoas muscle and abdominal aortic branch (Figs. 3D and E, respectively). Originally the cyst was deemed to be a neurofibroma, however, resection, additional pathological analysis and positives for Desmin, Myo-D1 and S-100 protein IHCs were more consistent with a diagnosis of MTT.

The patient was not subjected to post-excision chemotherapy and radiotherapy, although he experienced progressive dysuria for a period of five months. Upon re-examination of the chest and abdominal regions by CT scans, multiple irregular nodules and masses within the abdominal cavity and retroperitoneal space were observed, consistent with a diagnosis of the recurrence of MTT (Fig. 4A). Once again, it was apparent that changes in cyst morphology, necrosis, hemorrhage and presence of septate lesions were, therefore, characteristics unique to MTT tumorigenesis. We noted that resurgence of tissue mass after excision was accompanied by invasion of the perirenal spaces and blockage of both ureters resulting in pelvicalyceal dilatation and hydronephrosis by enlargement of nodules in the perinephric space (yellow arrow, Fig. 4B). Tumor embolus features in bilateral iliac veins, postcava and right atrium were also observed (red arrow, Fig. 4B). In post excision contrast-enhanced CT scans of the chest area, the large, 5.2 cm × 3.2 cm well-defined lobulate mass adjacent to the right-side pulmonary hilum (Fig. 4C) appeared to be unchanged from preoperative conditions (Figs. 3C, D and E). The patient was subsequently

discharged and the case followed up with a post clinical study. The two patients had been informed consent to publish this paper.

Discussion

MTTs account for 5% among MPNSTs which display different patterns of malignancy in areas of mesenchymal differentiation.^{3, 12} Of these, two subcategories are further refined according to clinical status of associated neurofibromatosis type 1 (NF-1).¹³⁻¹⁴ To date, definition of MTT etiology, pathogenesis and genetics is imprecise and identification of clinical symptoms is somewhat subjective depending upon the location, size and presence or absence of nerve compression and adjacent tissue metastasis. Prognosis for many MTT sufferers is certainly less favorable than for more classical MPNSTs especially, where a correct diagnosis must be accurately informed from familial and clinical history and knowledge of the complexities of individual MTT subtypes. Generally, a definitive diagnosis for an MTT is based upon observations from histological staining and true positives for S-100 protein, Myo-D1 and Desmin in post-surgical IHC assays.^{2-3, 8-9} Clinical histories of most patients with MTT cases typically range between several months to more than ten years in all age groups.¹⁵⁻¹⁶ In the two cases exemplified in this present work, the patient ages were 37 and 41 years, respectively. In both scenarios, MTTs arose in rare locations of lung and abdomen. Interestingly, two MTT subtypes were clearly distinguishable in CT imaging analyses and while affirmation in the younger male patient was also through a familial predisposition of NF-1, this was absent within the older female.

Diagnosis of MTTs is, at best, difficult prior to surgery and recent occurrence where imaging analyses were applied for reporting of the clinical manifestations of MTTs, are scarce.¹⁷⁻¹⁸ Owing to the diversity of these tumors, image features tend to be non-specific and low in descriptive clarity. In previous studies, CT imaging analyses revealed MTTs could be identified by the presence of a prominent discoid shadow with a well-circumscribed lobulated morphology. In addition, MTTs were invariably of an irregular shape and of higher density at the margin of the cystic mass in comparison to the majority of MPNSTs. On occasion, MTTs presented with some high density stripe-like entities distributed throughout the mass. Unfortunately, the structural characteristics of rhabdomyosarcomas are frequently ill-defined or generally unobserved within CT images. Although, it is plausible that some CT imaging features are masked or obscured in the presence of an abundant blood supply whereby the mass of the MTT increases rapidly and disproportionately within a short time frame or in the presence of a Schwann cell metaplasia of neural crest during a state high-malignancy.^{2, 19} On occasion, hemorrhage, necrosis and cystic morphological changes are observed in the lesions with a distinct high-density calcification shadow.²⁰⁻²¹ Importantly, contrast-enhanced CT scans enable mild enhancement of cyst peripheral features and thus, specificity of MTT classification based on cyst heterogeneity and linear or annular morphology of the septal shadow. Interestingly, some characteristics of MTTs including, hypointense mass and presence of septum-like structures on T1- and T2-weighted images were available from MRI studies as early as 2009¹ and these can be added with certainty to the repertoire of features typically observed within modern CT scans to increase accuracy for diagnosis of MTTs.

Conclusion

Accurate diagnosis to separate out MTTs from other conventional MPNSTs presents a paradox. Both present as a large soft tissue mass on image examination and conventional MPNSTs are also generally heterogeneous. Other image features in common include ill-defined margin, intratumoral lobulation, peritumoral edema, calcification lesions and destruction of adjacent bone tissues. For an accurate and rapid diagnosis of MTTs in the preoperative state, we have refined CT imaging analyses to reliably allow clear distinction between specific features from two unique clinical cases. We thereby present the first reliable clinical references features from CT analyses for diagnosis of MTTs based upon: (1) Enormity of mass-like shadow; (2) presence of well-circumscribed lobulated shape; (3) septum within the well-defined mass accompanied with hemorrhage, necrosis and cystic changes as well as calcification, especially within NF-1 patients. Whilst these may not be regarded as “golden standard”, they are prerequisite as indicators at an early clinical stage for the accurate diagnosis for differential MTTs.

Abbreviations

CT: Computed tomography; MTTs: Malignant triton tumors; IHC: Immunohistochemistry; MRI: Magnetic resonance imaging; NF-1: Neurofibromatosis type 1; MPNSTs: Malignant peripheral nerve sheath tumors; H&E: hematoxylin and eosin; BMI: Body mass index.

Declarations

Acknowledgments

Not applicable

Authors' contributions

LY, CZ and NJ collected clinical cases and made analysis; DPM, QP, CZ wrote and revised the manuscript; HS, DC and QC took part to the patient therapy. All authors read and approved the final manuscript.

Funding

This study was supported by the Medical Scientific Youth Project of Chongqing Municipal Health and Family Planning Commission of China (No. 2018QNXM004), Education and Teaching Research Project of Chongqing Medical University (No. JY180321), Science and Technology Research Project of Chongqing Education Commission (No. KJQN201900425), and National Natural Science Foundation of China (No. 81972023).

Availability of data and materials

The datasets used during the current study are available from the corresponding author on reasonable request

Ethics approval and consent to participate

The study was approved by the Ethics Committee of the First Affiliated Hospital of Chongqing Medical University. Both patients in this prospective study signed a written informed consent, which included the agreement for scientific use of their data.

Consent for publication

Not applicable.

Conflict of interest

The authors declare no conflict of interest.

Author details

^a Department of Cardiothoracic Surgery, the First Affiliated Hospital of Chongqing Medical University, Chongqing 400016, China. ^b Department of Radiology, the First Affiliated Hospital of Chongqing Medical University, Chongqing 400016, China. ^c Department of Pathology, Chongqing Medical University, Chongqing 400016, China. ^d School of Basic Medical Science, Chongqing Medical University, Chongqing 400016, China

References

1. Dartnell, J.; Pilling, J.; Ferner, R.; Cane, P.; Langlazdunski, L., Malignant Triton Tumor of the Brachial Plexus Invading the Left Thoracic Inlet: A Rare Differential Diagnosis of Pancoast Tumor. *J. Thorac. Oncol.* **2009**, *4* (1), 135-137.
2. Bishop, J. A.; Thompson, L. D. R.; Cardesa, A.; Barnes, L.; Lewis, J. S.; Triantafyllou, A.; Hellquist, H.; Stenman, G.; Hunt, J. L.; Williams, M. D., Rhabdomyoblastic Differentiation in Head and Neck Malignancies Other Than Rhabdomyosarcoma. *Head Neck Pathol.* **2015**, *9* (4), 507-518.
3. Stasik, C. J.; Tawfik, O., Malignant peripheral nerve sheath tumor with rhabdomyosarcomatous differentiation (malignant triton tumor). *Arch. Pathol. Lab. Med.* **2009**, *130* (12), 1878-1881.
4. Brooks, J. J.; Freeman, M.; Enterline, H. T., Malignant "Triton" tumors. Natural history and immunohistochemistry of nine new cases with literature review. *Cancer* **1985**, *55* (11), 2543-2549.
5. Kamperis, E.; Barbetakis, N.; Asteriou, C.; Kleontas, A.; Christoforidou, Malignant triton tumor of the chest wall invading the lung. A case report and literature review. *Hippokratia* **2013**, *17* (3), 277.
6. Li, G.; Liu, C.; Liu, Y.; Xu, F.; Su, Z.; Wang, Y.; Ren, S.; Deng, T.; Huang, D.; Tian, Y., Analysis of clinical features and prognosis of malignant triton tumor: A report of two cases and literature review. *Oncol. Lett.* **2015**, *10* (6), 3551-3556.
7. Mcconnell, Y. J.; Giacomantonio, C. A., Malignant triton tumors-complete surgical resection and adjuvant radiotherapy associated with improved survival. *J. Surg. Oncol.* **2012**, *106* (1), 51-56.

8. Chaudhry, I.; Algazal, T.; Cheema, A.; Faraj, A. A.; Malki, N. A.; Mutairi, H.; Abbas, A.; Amr, S. S., Mediastinal malignant triton tumor: a rare case series and review of literature. *Int. J. Surg. Case Rep.* **2019**, *62*, 115-119.
9. Gao, L.; Song, H.; Mu, K.; Wang, J.; Guo, B.; Shi, B.; Li, G., Primary epididymis malignant triton tumor: case report and review of the literature. *Eur. J. Med. Res.* **2015**, *20* (1), 79-79.
10. Zakzouk, A.; Hammad, F.; Langlois, O.; Aziz, M.; Marie, J. P.; Choussy, O., Malignant triton tumour of the sinonasal tract: Case report and literature review. *Int. J. Surg. Case Rep.* **2014**, *5* (9), 608-612.
11. Woodruff, J. M.; Chernik, N. L.; Smith, M. C.; Millett, W. B.; Foote, F. W., Peripheral nerve tumors with rhabdomyosarcomatous differentiation (malignant "Triton" tumors). *Cancer* **1973**, *32* (2), 426-439.
12. Kamran, S. C.; Shinagare, A. B.; Howard, S. A.; Hornick, J. L.; Ramaiya, N. H., A-Z of malignant peripheral nerve sheath tumors. *Cancer Imaging* **2012**, *12* (3), 475-483.
13. Jaing, T.; Chuang, C.; Jung, S.; Wu, C.; Tseng, C.; Chen, C., Malignant Triton Tumor of the Cervical Spine: Report of One Case and Review of the Literature. *Pediatr. Neonatol.* **2015**, *56* (1), 58-61.
14. Farid, M.; Demicco, E. G.; Garcia, R.; Ahn, L.; Merola, P. R.; Cioffi, A.; Maki, R. G., Malignant peripheral nerve sheath tumors. *Oncologist* **2014**, *19* (2), 193-201.
15. Aldlyami, E.; Dramis, A.; Grimer, R. J.; Abudu, A.; Carter, S. R.; Tillman, R. M., Malignant triton tumour of the thigh-a retrospective analysis of nine cases. *Eur. J. Surg. Oncol.* **2006**, *32* (7), 808-810.
16. Tish, S.; Ross, L.; Habboub, G.; Roser, F.; Recinos, P. F., Malignant triton tumor diagnosed twelve years after radiosurgically treated vestibular schwannoma. *Clin. Neurol. Neurosurg.* **2019**, *183*, 105367.
17. Han, D. H.; Kim, D. G.; Chi, J. G.; Park, S.; Jung, H.; Kim, Y. G., Malignant triton tumor of the acoustic nerve: Case report. *J. Neurosurg.* **1992**, *76* (5), 874-877.
18. Nosaka, S.; Kao, S. C., MRI of malignant "Triton" tumor in a child. *Clinical Imaging* **1993**, *17* (1), 53-55.
19. Allen, S. D.; Moskovic, E.; Fisher, C.; Thomas, J. M., Adult rhabdomyosarcoma: cross-sectional imaging findings including histopathologic correlation. *Am. J. Roentgenol.* **2007**, *189* (2), 371-377.
20. Langlazdunski, L.; Pons, F.; Jancovici, R., Malignant "Triton" tumor of the posterior mediastinum: prolonged survival after staged resection. *Ann. Thorac. Surg.* **2003**, *75* (5), 1645-1648.
21. Kamran, S. C.; Shinagare, A. B.; Howard, S. A.; Nishino, M.; Hornick, J. L.; Krajewski, K. M.; Ramaiya, N. H., Intrathoracic Malignant Peripheral Nerve Sheath Tumors: Imaging Features and Implications for Management. *Radiol. Oncol.* **2013**, *47* (3), 230-238.

Figures

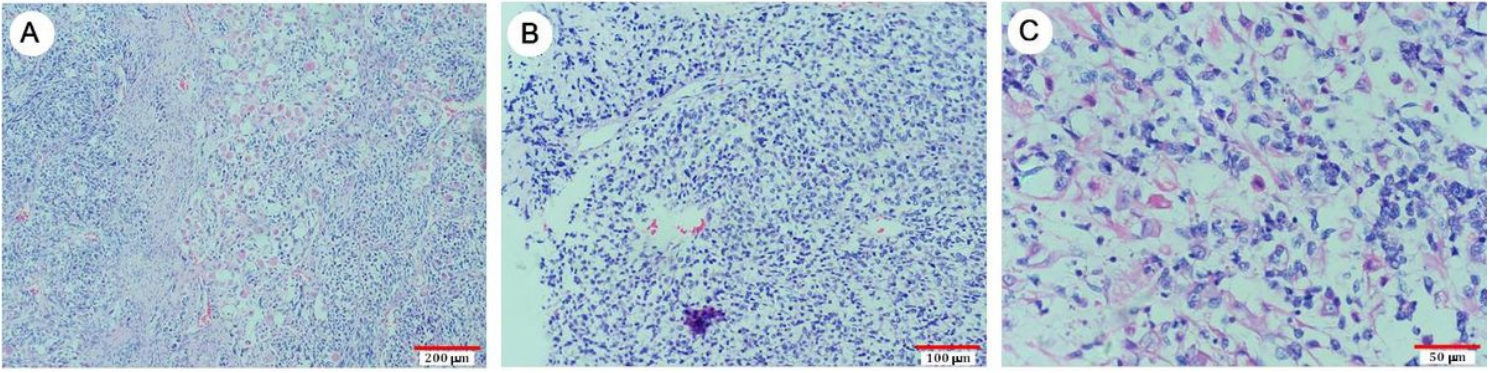


Figure 1

Representative H&E staining of tumor on 41-year-old female MTT-suspected patient in postoperative course, who was admitted to our hospital. (A) original magnification 50x; (B) 100x; (C) 200x.

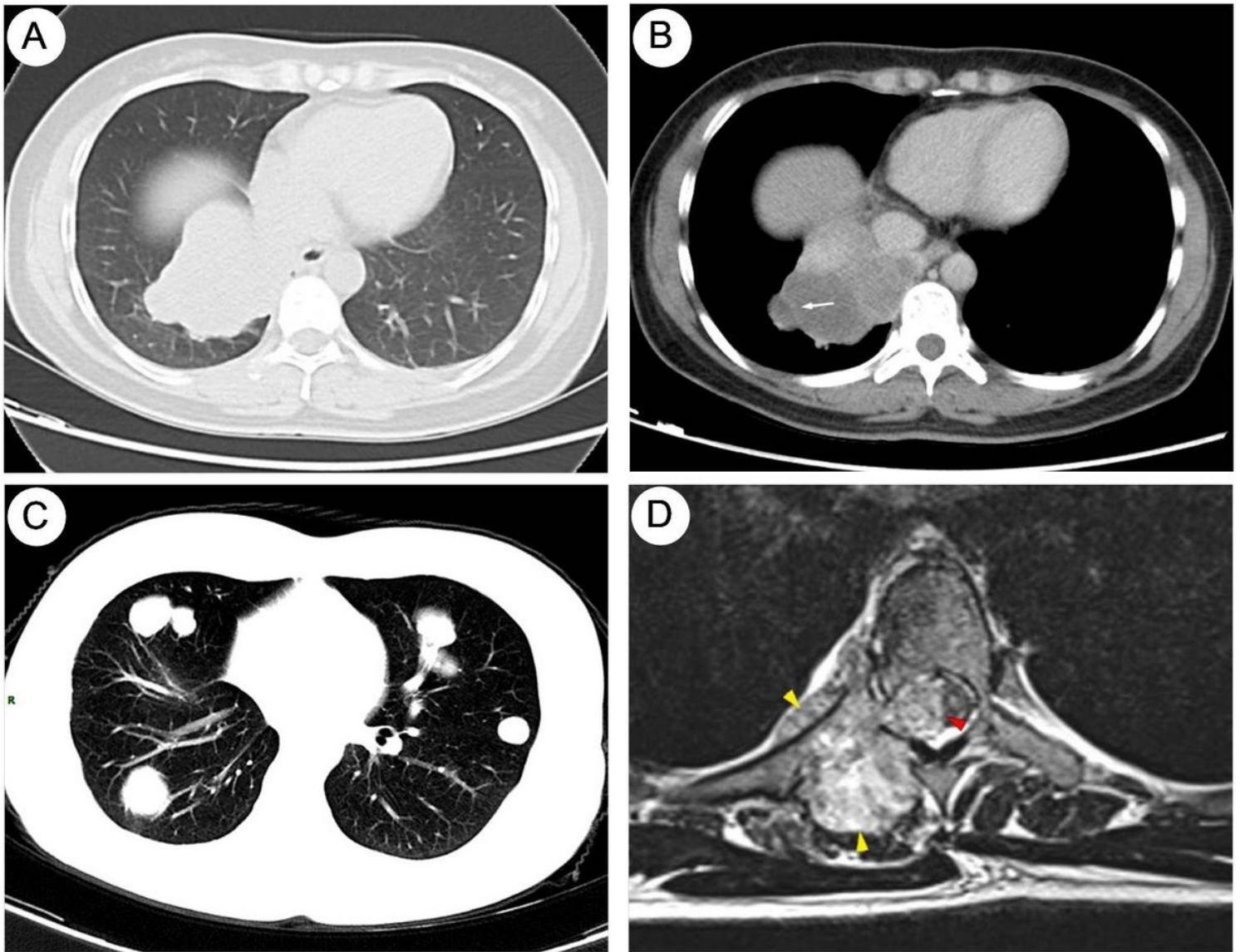


Figure 2

CT and MRI images of a 41-year-old female patient with complains of respiratory distress and shortness of breath. (A) Chest CT images shows that a huge irregular and well-defined mass in medial basal segment of lower lobe of right lung. (B) Contrast-enhanced chest CT scan in delayed phase illustrates a mass-like shadow with a mediastinal window, which has irregular and well-circumscribed lobulated shape. Low-density cystic mass is obvious at the margin of the lesion, as illustrated by white arrow. (C) Five months later, chest CT scan displays multiple well-defined nodules and masses in bilateral lungs, suggesting recurrence and metastasis of MTTs. (D) MRI image indicates that a tissue mass with homogeneous density grows in the vertebral index at T4-T5 thoracic segments (T4-T5), along with microbleeds.

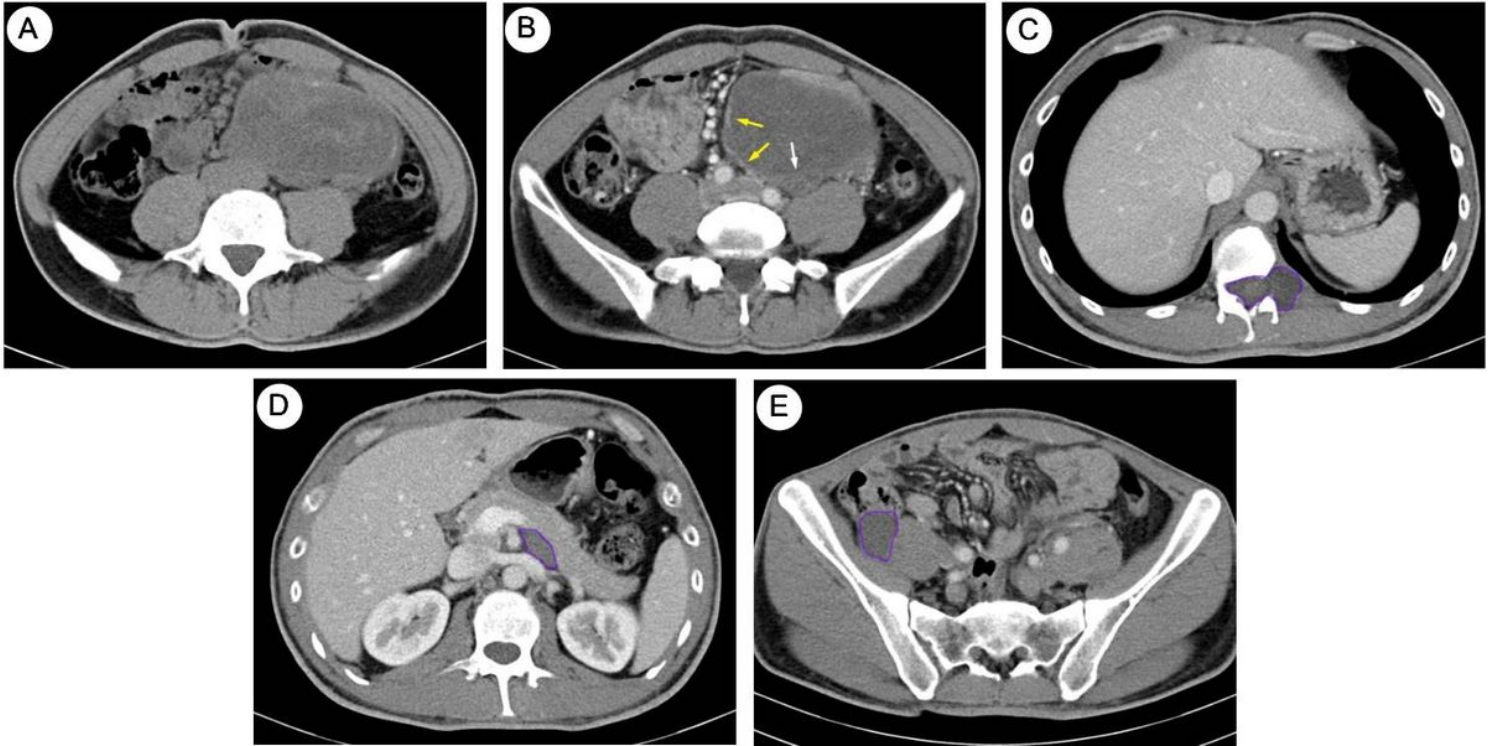


Figure 3

CT images of a 37-year-old male patient with a family history of NF-1. (A) The abdominal CT scan shows an enormous mass was in abdominal cavity. It is obvious that calcifications have occurred at the margin of mass shadow. (B) By contrast-enhanced CT scan, linear septum (white arrow) and partial edge (yellow arrows) are clear with abdominal window, respective. In addition, A few hypodense nodules (purple circles) appears: (C) between the T12 and L1; (D) behind the pancreas body; and (E) beside the right iliopsoas muscle, respectively.



Figure 4

Five months after radical mass excision, the 37-year-old male has complained of dysuria. (A) Contrast-enhanced abdominal CT scan shows multiple irregular nodules and masses in abdominal cavity and retroperitoneal spaces. (B) It is observed that reappeared mass grows into the perirenal spaces and blocks ureters on both sides, which give rise to pelvicalyceal dilatation and hydronephrosis, outlined by yellow arrow. And we can see tumor embolus in bilateral iliac veins, postcava and right atrium shown by red arrow. (C) Chest CT scan demonstrates a huge well-defined mass appears adjacent to the right-side pulmonary hilum with a mediastinal window.